Spin and Parity Analysis in the Double-Regge Model*

C. D. Froggatt†
Niels Bohr Institute, Copenhagen, Denmark

and

G. Ranft
Sektion Physik, Karl Marx Universität, Leipzig, Germany
(Received 30 November 1971; revised manuscript received 10 January 1972)

The formalism is given for a partial-wave analysis of a low-mass two-body subsystem produced via a double-Regge amplitude at small momentum transfer. This method is applied to the Reggeized Deck amplitude for the reaction $\pi N \to \rho\pi N$ in the ρ-π mass region of the A enhancement. At lower mass values the results are less sensitive to the exact form of the pion Regge trajectory, and about 75–80% of the cross section in the A_1 region is given by a 1^+ S-wave ρ-π state. This amplitude is largely real and the Argand diagrams for the partial waves do not show resonant structure. However, phenomenologically it is difficult to distinguish between the Berger amplitude and an A_1-resonance production amplitude. The spin-parity decomposition in the A_2 mass region is also discussed.

I. INTRODUCTION

It is well known that the double peripheral model and, in particular, the double-Regge model predict invariant-mass-squared distributions $\partial\sigma/\partial s_i$ which are peaked at small invariant mass. For example, in the reaction $\pi N \to \rho\pi N$ a distribution $\partial\sigma/\partial s_{\rho\pi}$ strongly peaked at small values of the ρ-π invariant energy squared $s_{\rho\pi}$ was obtained by Deck,[1] who considered elementary pion exchange and diffraction scattering. Berger[2] has repeated Deck's calculation with Reggeized pion exchange and diffraction scattering represented by a flat Pomeranchon exchange. The general features of the data for production of a low-mass ρ-π state are reproduced by Berger's amplitude, apart from A_2 production at lower incident pion energies.

Extending the concept of duality from two-body processes[3] to production amplitudes, Chew and Pignotti[4] argued that the low-mass enhancement from the Deck effect should be interpreted as predicting the existence of a ρ-π resonance, i.e., the A_1 resonance. It has since been realized that π exchange, being mainly real, cannot be semilocally dual to a resonance-dominated description of the A_1 bump, which gives a mainly imaginary amplitude. In order to satisfy the finite-energy sum rule (FESR), the A_1 resonance would have to be narrow or weakly produced compared with the observed 3π mass distribution. We note that, in the successful application[5] of FESR using the imaginary part of π exchange for ρ photoproduction, the Reggeized Drell term yields a much broader cross section than the experimental 2π mass distribution and is about eight times smaller at the ρ peak.

Here we wish to study the structure of the double-Regge amplitude at low subenergy in more detail. In particular we want to compare the partial-wave decomposition with that expected for resonance production.

We are interested in double-Regge-exchange graphs, which contribute significantly in the region where one particular two-particle subsystem is produced with low invariant mass at small momentum transfer squared, say t_2. For these graphs, the momentum-transfer-squared variable t_2 can be considered as replacing the mass of an external particle in a quasi-two-body reaction. In Sec. II the formalism for performing a partial-wave analysis of the corresponding double-Regge amplitude, in the center of mass of the two-body subsystem, is developed in detail.

The ρ-π subsystem in the process $\pi N \to \rho\pi N$ is treated as a particular case in Sec. III. A short account of this work has already been published.[6] We only consider the single Reggeized Deck graph, which is known to give a good average fit to the data. We use the asymptotic form of the amplitude available in the literature[2] with the conventional Regge phase. For other reactions, the multi-Veneziano model[7,8] or the Chan-Łoskiewicz-Allison (CŁA) multi-Regge model and its extensions[9] are more successful. Some multiperipheral bootstrap calculations and estimates on cross sections for production processes[10-12] also assume that the multi-Regge model approximately holds in

the whole of phase space. It is, therefore, important to study in what detail the multi-Regge amplitude represents the production dynamics at small invariant subenergies.

In Sec. IV we discuss the results of our partial-wave analysis for the Deck process $\pi N \to \rho\pi N$. It is found that the system produced in the A_1 mass region is predominantly produced in a 1^+ S-wave state. This could also be expected in the case of dominant resonance production. The Reggeized Deck amplitude is largely real (i.e., nonabsorptive) in this mass interval and the Argand diagrams for the most important partial waves do not show evidence for resonant structure. However, phenomenologically, it is difficult to determine the behavior of the phase of the 1^+ S-wave at the A_1 mass. So, at present, it is not possible to say whether the Berger amplitude or a dominantly resonant amplitude is the correct physical description. We also consider the partial-wave structure at higher invariant masses, including the A_2 region.

II. SPIN STRUCTURE OF THE DOUBLE-REGGE AMPLITUDE

In this section we present the formalism to perform a partial-wave analysis of the two-particle (1, 2) subsystem for a double-Regge expansion of the three-body production process

$$a+b \to 1+2+3 \tag{2.1}$$

shown in Fig. 1. The spin-parity decomposition is made in the Gottfried-Jackson[13] frame for the subsystem.

For the process (2.1), we denote the four-momentum, mass, spin, and parity of particle i by p_i, m_i, J_i, and η_i^p, respectively, and choose the set of five invariants

$$s=(p_a+p_b)^2, \quad s_1=(p_1+p_2)^2, \quad s_2=(p_2+p_3)^2,$$
$$t_1=(p_a-p_1)^2, \quad \text{and} \quad t_2=(p_b-p_3)^2. \tag{2.2}$$

Following Bali, Chew, and Pignotti,[14] we make a double O(2, 1) expansion of the three-particle production amplitude

$$\hat{f}_{\mu_3\lambda_2\lambda_1,\lambda_a\mu_b}(s, s_1, s_2, t_1, t_2; \omega)$$

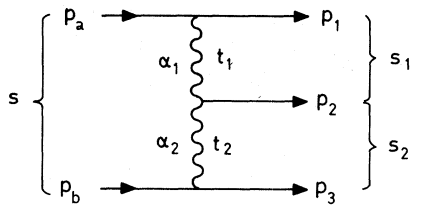

FIG. 1. The double-Regge graph corresponding to the direct-channel process $a+b \to 1+2+3$.

in the s-channel physical region. The expansion variables are the two boost parameters $2\zeta^{12}$ and $2\zeta^{23}$ given by

$$\cosh 2\zeta^{12} = \frac{-2t_1(s_1-t_2-m_a^2)-(m_1^2-m_a^2-t_1)(m_2^2-t_1-t_2)}{[\lambda(t_1, m_a^2, m_1^2)\lambda(t_1, t_2, m_2^2)]^{1/2}}, \tag{2.3}$$

$$\cosh 2\zeta^{23} = \frac{-2t_2(s_2-t_1-m_b^2)-(m_3^2-m_b^2-t_2)(m_2^2-t_1-t_2)}{[\lambda(t_2, m_b^2, m_3^2)\lambda(t_1, t_2, m_2^2)]^{1/2}}, \tag{2.4}$$

where

$$\lambda(x, y, z)=x^2+y^2+z^2-2xy-2yz-2zx \tag{2.5}$$

and ω is the Toller angle[14,15] ($-\pi \leq \omega \leq \pi$). For later discussion we list the Toller angle ω, which is a double-valued function of the invariants $\omega=\omega(s, s_1, s_2, t_1, t_2)$, among the arguments of the amplitude. The helicity labels $\lambda_a, \lambda_1, \lambda_2$ for particles a, 1, and 2 refer to the s_1 brick-wall frame[16] in which p_a-p_1 is along the z axis, and the helicitiy labels μ_b and μ_3 for particles b and 3 refer to the s_2 brick-wall frame, in which p_b-p_3 is along the z axis.

Crossing symmetry may be used[16] to introduce the O(2, 1) helicity amplitude

$$f_{\bar{\mu}_b\mu_3\lambda_2,\lambda_a\bar{\lambda}_1}=\sum_{\lambda_1,\mu_b} D^{J_1}_{\lambda_1\bar{\lambda}_1}(C)D^{J_b}_{\mu_b\bar{\mu}_b}(C^{-1})\,\hat{f}_{\mu_3\lambda_2\lambda_1,\lambda_a\mu_b}, \tag{2.6}$$

which can be identified with an appropriate analytic

continuation of the crossed-t_1-and-t_2-channel helicity amplitude of Wick.[17] The spinor lowering operator C corresponds to a rotation by π:

$$D^J_{\lambda\lambda'}(C) = (-1)^{J+\lambda}\delta_{\lambda,-\lambda'}. \tag{2.7}$$

Our helicity phase conventions are chosen to agree with those of Ref. 17. In particular, when we cross this O(2, 1) helicity amplitude to the s_1 center-of-mass system, we obtain the usual Trueman and Wick crossing matrix[18] for particles a, 1, and 2.

The O(2, 1) harmonic expansion of f gives

$$f_{\bar{\mu}_b\mu_3\lambda_2,\lambda_a\bar{\lambda}_1}(s, s_1, s_2, t_1, t_2; \omega) = \sum_{\mu}\int_{-\frac{1}{2}-i\infty}^{-\frac{1}{2}+i\infty} dj_1 \int_{-\frac{1}{2}-i\infty}^{-\frac{1}{2}+i\infty} dj_2 F^{j_1 j_2 \mu}_{\bar{\mu}_b\mu_3\lambda_2,\lambda_a\bar{\lambda}_1}(t_1, t_2) d^{j_1}_{\lambda_a-\bar{\lambda}_1,\mu-\lambda_2}(\cosh 2\zeta^{12}) \exp(i\mu\omega) d^{j_2}_{\mu,\bar{\mu}_b-\mu_3}(\cosh 2\zeta^{23}), \tag{2.8}$$

which can be identified with an appropriate analytic continuation of the crossed-channel expansion of Ref. 17. When both ζ^{12} and ζ^{23} are large, the asymptotic behavior is governed by the leading singularities in j_1 and j_2. We assume these singularities are boson Regge-pole trajectories $\alpha_1(t_1)$ and $\alpha_2(t_2)$, having signatures τ_1 and τ_2 and physical states of parity P_1 and P_2, respectively, to obtain the asymptotic factorized double-Regge amplitude[14,15]

$$f_{\bar{\mu}_b\mu_3\lambda_2,\lambda_a\bar{\lambda}_1}(s, s_1, s_2, t_1, t_2; \omega) = \sum_{\mu} h_{\bar{\lambda}_1\lambda_a}(t_1) h_{\mu_3\bar{\mu}_b}(t_2) h_{\lambda_2\mu}(t_1, t_2) \exp(i\mu\omega) d^{\alpha_1}_{\lambda_a-\bar{\lambda}_1,\mu-\lambda_2}(\cosh 2\zeta^{12}) d^{\alpha_2}_{\mu,\bar{\mu}_b-\mu_3}(\cosh 2\zeta^{23}) \tag{2.9}$$

$$= \eta_1(t_1)\eta_2(t_2)\exp\{\tfrac{1}{2}[-i\pi(\lambda_a-\bar{\lambda}_1+\lambda_2-\bar{\mu}_b+\mu_3)]\}\gamma_{\bar{\lambda}_1\lambda_a}(t_1)\gamma_{\mu_3\bar{\mu}_b}(t_2)\gamma_{\lambda_2}(t_1, t_2, \omega)[(s_1\cdots)/s_0]^{\alpha_1}[(s_2\cdots)/s_0]^{\alpha_2}. \tag{2.10}$$

In this expression, the quantities $(s_1\cdots)$ and $(s_2\cdots)$ are the numerators of the $\cosh 2\zeta^{12}$ and $\cosh 2\zeta^{23}$ variables and are explicitly

$$(s_1\cdots) = s_1 - t_2 - m_a^2 + \tfrac{1}{2}t_1^{-1}(m_1^2 - m_a^2 - t_1)(m_2^2 - t_1 - t_2), \tag{2.11}$$

$$(s_2\cdots) = s_2 - t_1 - m_b^2 + \tfrac{1}{2}t_2^{-1}(m_3^2 - m_b - t_2)(m_2^2 - t_1 - t_2). \tag{2.12}$$

The corresponding denominators are absorbed into the vertex functions γ_{ij} and γ_{λ_2} and the parameter s_0 is an arbitrary scale factor. We retain $(s_1\cdots)^{\alpha_1}$ rather than $s_1{}^{\alpha_1}$, since the former is most often used in Reggeized double-peripheral-model calculations[2] involving pion exchange. The complicated question of kinematic singularities[19] and nonasymptotic corrections is not discussed here. We assume that the phase of the multi-Regge amplitude is given by the product of the conventional signature factors[20]

$$\eta_i(t) = [\tau_i + \exp(-i\pi\alpha_i)]/\sin\pi\alpha_i \tag{2.13}$$

for the trajectories α_1 and α_2. Note that we also exhibit explicitly the asymptotic phase from the O(2, 1) representation functions in our Regge amplitude (2.10).

The parity transformation properties[17,21] of the vertex functions for the coupling of the Regge pole $\alpha(t)$ to the particles m and n and for the coupling of two Regge poles $\alpha_1(t_1)$ and $\alpha_2(t_2)$ to particle r are

$$\gamma_{\lambda_m\lambda_n}(t) = N_{mn\alpha}\gamma_{-\lambda_m-\lambda_n}(t), \tag{2.14}$$

$$\gamma_{\lambda_r}(t_1, t_2, \omega) = N_{r\alpha_1\alpha_2}\gamma_{-\lambda_r}(t_1, t_2, -\omega). \tag{2.15}$$

Here the normalities associated with the vertices are given by

$$N_{mn\alpha} = (-1)^{J_m+J_n}\eta^p_m\eta^p_n\tau_\alpha P_\alpha, \tag{2.16}$$

$$N_{r\alpha,\alpha_2} = (-1)^{J_r}\eta^p_r\tau_1 P_1\tau_2 P_2. \tag{2.17}$$

We want to make a partial-wave analysis of the (1, 2) subsystem, at small values of the squared subenergy s_1 for fixed total energy squared s and fixed small values of the momentum transfer squared t_2. So we apply crossing symmetry to transform the O(2, 1) helicity amplitude to the system where the helicities of particles a, 1, and 2 are referred to the center-of-mass frame of particles 1 and 2. However we retain the O(2, 1) helicity labels for particles b and 3. The crossing matrix[18] for particles a, 1, and 2 can be calculated by treating the crossed process as a quasi-two-body reaction (see Fig. 2)

$$a + \bar{1} \to (\bar{b}+3) + 2, \tag{2.18}$$

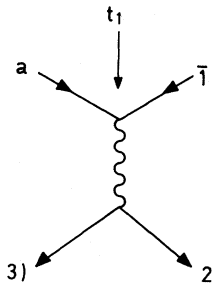

FIG. 2. The quasi-two-body reaction $a+\bar{1}\to(\bar{b}+3)+2$.

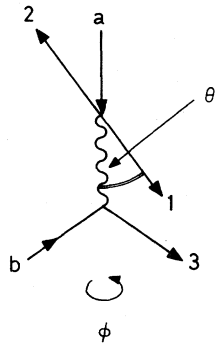

FIG. 3. The reaction $a+b\to 1+2+3$ in the (1,2) subsystem rest frame. θ is the Jackson angle between particles a and 1 in the (1,2) rest frame, and ϕ is the Treiman-Yang angle.

using the phase conventions of Jacob and Wick.[21] The corresponding Wigner rotations associated with particles b and 3 give a phase factor $\exp[i(\vec{\mu}_b-\mu_3)\psi]$, where $\psi\to 0$ asymptotically and is neglected in the following analysis. Hence we obtain the s_1 center-of-mass helicity amplitudes

$$H_{\vec{\mu}_b\mu_3\lambda_2\lambda_1,\lambda_a}(s,s_1,s_2,t_1,t_2)=\sum_{\lambda_a',\bar{\lambda}_1,\lambda_2'} d^{J_a}_{\lambda_a\lambda_a'}(\chi_a)\,d^{J_1}_{\lambda_1\bar{\lambda}_1}(\chi_1)\,d^{J_2}_{\lambda_2\lambda_2'}(\chi_2)\times\exp[-i\pi(\lambda_a'+\bar{\lambda}_1+\lambda_2'-J_1)]f_{\vec{\mu}_b\mu_3\lambda_2',\lambda_a'\bar{\lambda}_1},\tag{2.19}$$

where we have neglected a possible constant helicity-independent crossing phase factor.

No analytic continuation is involved in this expression. We have associated the conventional "particle two" phase factor with particle 2, and the scattering angle θ [see Eq. (2.26)] for particle 1 satisfies $0\le\theta\le\pi$. The crossing angles χ_i are given[18] in terms of the invariants for the quasi-two-body process (2.18) by

$$\cos\chi_a=\frac{(t_1+m_a^2-m_1^2)(s_1+m_a^2-t_2)-2m_a^2\Delta}{[\lambda(t_1,m_a^2,m_1^2)\lambda(s_1,m_a^2,t_2)]^{1/2}},\tag{2.20}$$

$$\cos\chi_1=\frac{-(t_1-m_a^2+m_1^2)(s_1+m_1^2-m_2^2)-2m_1^2\Delta}{[\lambda(t_1,m_a^2,m_1^2)\lambda(s_1,m_1^2,m_2^2)]^{1/2}},\tag{2.21}$$

$$\cos\chi_2=\frac{(t_1+m_2^2-t_2)(s_1+m_2^2-m_1^2)-2m_2^2\Delta}{[\lambda(t_1,t_2,m_2^2)\lambda(s_1,m_1^2,m_2^2)]^{1/2}},\tag{2.22}$$

where we take $0\le\chi_i\le\pi$,

$$\Delta=m_a^2-t_2-m_1^2+m_2^2,\tag{2.23}$$

and $\lambda(x,y,z)$ is defined in Eq. (2.5).

The s_1 center-of-mass system introduced above is related to the (1, 2) Jackson frame[13] shown in Fig. 3 by the Treiman-Yang rotation ϕ[13,22] about the z axis (i.e., the direction of motion of particle a). We remark here that the Treiman-Yang angle ϕ is different from the Toller angle ω mentioned earlier and is given by

$$\cos\phi=\left.\frac{(\vec{p}_a\times\vec{p}_1)\cdot(\vec{p}_b\times\vec{p}_3)}{|\vec{p}_a\times\vec{p}_1||\vec{p}_b\times\vec{p}_3|}\right|_{\vec{p}_1+\vec{p}_2=0}\tag{2.24}$$

$$=\frac{N(s,s_1,s_2,t_1,t_2)}{[D_1(s_1,t_1,t_2)D_2(s,s_1,t_2)]^{1/2}}.\tag{2.25}$$

Expressions for N, D_1, and D_2 are given in the Appendix, Eqs. (A3)–(A7). The sign of $\sin\phi$ is not determined by the invariants and is directly related to that of the Toller angle ω in Eq. (2.10). The Jackson angle θ can also be expressed in terms of invariants by

$$\cos\theta=\left.\frac{\vec{p}_a\cdot\vec{p}_1}{|\vec{p}_a||\vec{p}_1|}\right|_{\vec{p}_1+\vec{p}_2=0}\tag{2.26}$$

$$=\frac{s_1^2+s_1(2t_1-t_2-m_a^2-m_1^2-m_2^2)+(m_a^2-t_2)(m_1^2-m_2^2)}{[\lambda(s_1,t_2,m_a^2)\lambda(s_1,m_1^2,m_2^2)]^{1/2}}.\tag{2.27}$$

We now make Wigner projections in the Jackson frame onto states of the (1, 2) subsystem with definite angular momentum J and parity P.[21,23] If neither λ_1 nor λ_2 is zero, the amplitudes of angular momentum J, with component M along the direction of motion of particle a, and the normality $N=(-1)^JP=\pm1$ are

$$a^{JM\pm}_{\bar{\mu}_b\mu_3\lambda_2\lambda_1,\lambda_a}(s, s_1, t_2)$$
$$= [(2J+1)/8\pi]^{1/2} \int_{-1}^{1} d\cos\theta \int_0^{2\pi} d\phi \exp[i(\lambda_a - M)\phi][d^J_{M\lambda_{12}}(\theta) H_{\bar{\mu}_b\mu_3\lambda_2\lambda_1,\lambda_a} \pm N_{12} d^J_{M-\lambda_{12}}(\theta) H_{\bar{\mu}_b\mu_3-\lambda_2-\lambda_1,\lambda_a}]. \quad (2.28)$$

Here $\lambda_{12} = \lambda_1 - \lambda_2 \geq 0$ and $N_{12} = (-1)^{J_1+J_2-V_1}\eta_1^b\eta_2^b$, where $V_1 = \frac{1}{2}$ if particle 1 is a fermion and $V_1 = 0$ for a boson. Since we neglect baryon exchange, particle 2 must be a boson. If $\lambda_1 = \lambda_2 = 0$ it is only possible to form states of normality $N = N_{12}$, the two terms in Eq. (2.28) become equal, and we have to multiply by an extra factor of $2^{-1/2}$ to obtain the correct normalization,

$$a^{JM,N_{12}}_{\bar{\mu}_b\mu_300,\lambda_a}(s, s_1, t_2) = [(2J+1)/4\pi]^{1/2} \int_{-1}^{1} d\cos\theta \int_0^{2\pi} d\phi \exp[i(\lambda_a - M)\phi] d^J_{M0}(\theta) H_{\bar{\mu}_b\mu_300,\lambda_a}. \quad (2.29)$$

In the following section we shall assume that the double-Regge amplitude is an even function of the Toller angle ω (in fact we shall follow the common procedure of neglecting all dependence of γ_{λ_2} on the angle ω). This is of course a dynamical assumption which remains to be tested; for $\lambda_2 = 0$ it is readily seen from Eq. (2.15) that this corresponds to neglecting couplings with normality change at the middle vertex.

Equivalently it follows that our amplitude H is an even function of $\sin\phi$, the Treiman-Yang angle of Eq. (2.24). In Eqs. (2.28)–(2.29) we integrate over the physical region of the invariants s_2 and t_1 twice, corresponding to positive and negative values of $\sin\phi$. For amplitudes even in $\sin\phi$, these two parts of the intergration become equal and we have

$$a^{JM\pm}_{\bar{\mu}_b\mu_3\lambda_2\lambda_1,\lambda_a}(s, s_1, t_2) = [(2J+1)/2\pi]^{1/2} \int_{t_1^{\min}}^{t_1^{\max}} dt_1 \int_{s_2^{\min}}^{s_2^{\max}} ds_2 J(s, s_1, s_2, t_1, t_2) \cos(M - \lambda_a)\phi$$
$$\times [d^J_{M\lambda_{12}}(\theta) H_{\bar{\mu}_b\mu_3\lambda_2\lambda_1,\lambda_a} \pm N_{12} d^J_{M-\lambda_{12}}(\theta) H_{\bar{\mu}_b\mu_3-\lambda_2-\lambda_1,\lambda_a}]. \quad (2.30)$$

Again for $\lambda_1 = \lambda_2 = 0$ we have to multiply by an extra factor of $2^{-1/2}$ to obtain the correct normalization,

$$a^{JM,N_{12}}_{\bar{\mu}_b\mu_300,\lambda_a}(s, s_1, t_2) = [(2J+1)/\pi]^{1/2} \int_{t_1^{\min}}^{t_1^{\max}} dt_1 \int_{s_2^{\min}}^{s_2^{\max}} ds_2 J(s, s_1, s_2, t_1, t_2) \cos(M - \lambda_a)\phi\, d^J_{M0}(\theta) H_{\bar{\mu}_b\mu_300,\lambda_a}. \quad (2.31)$$

Expressions for $\cos\phi$ and $\cos\theta$ in terms of invariants are given in Eqs. (2.25)–(2.27), while those for $t_1^{\min}$, $t_1^{\max}$, $s_2^{\min}$, $s_2^{\max}$, and the Jacobian $J(s, s_1, s_2, t_1, t_2)$ are given in the Appendix [Eqs. (A8)–(A12)]. For $\lambda_a = 0$ the double-Regge amplitude, Eq. (2.10), gives helicity partial-wave amplitudes which satisfy

$$a^{JM\pm}_{\bar{\mu}_b\mu_3\lambda_2\lambda_1,0} = \pm(-1)^M N_{a\alpha_2} a^{J-M\pm}_{\bar{\mu}_b\mu_3\lambda_2\lambda_1,0}, \quad (2.32)$$

where $N_{a\alpha_2} = (-1)^{J_a - V_a}\tau_2 P_2$.

The cross section for fixed values of the helicities[24] λ_i and μ_i is given in terms of the helicity partial-wave amplitudes by

$$\frac{\partial^2\sigma}{\partial s_1 \partial t_2} = C \sum_{J,M,\pm} |a^{JM\pm}_{\bar{\mu}_b\mu_3\lambda_2\lambda_1,\lambda_a}|^2, \quad (2.33)$$

where

$$C = \frac{[\lambda(s_1, m_1^2, m_2^2)]^{1/2}}{2^5(2\pi)^4 s_1 \lambda(s, m_a^2, m_b^2)}. \quad (2.34)$$

The amplitudes defined in Eqs. (2.28)–(2.31) can be readily transformed from the helicity basis into partial waves of definite orbital angular momentum L and resultant spin S.[21] If the (1, 2) subsystem does not interact with the third final-state particle 3, one expects[25] the physical partial-wave amplitudes for the reaction (2.1) to have the same phase dependence on the variable s_1 as the (1, 2) elastic scattering amplitude, provided the square of the energy s_1 is such that the inelasticity is small. In particular, if a resonant (1, 2) final state is dominant, then the corresponding partial-wave amplitude should be proportional to the Watson factor[25,26]

$$\exp(i\delta)\sin\delta/(q_{12})^{L+1}$$

and give anticlockwise loops in an Argand diagram. Here δ is the resonant phase shift, L is the orbital angular momentum associated with the partial wave, and q_{12} is the momentum of particle 1(2) in the s_1 center-of-mass system. If all the partial waves for a given spin-parity, J^P, are dominated by resonance production at some value of the squared subenergy s_1, then factorization implies that the ratios of the various partial waves with the allowed (L, S) values are the same for all values of the spin component M.

III. APPLICATION TO THE REACTION $\pi N \to \rho\pi N$

The double-Regge amplitudes expected to contribute to the processes

$$\pi^+ p \to \rho^0 \pi^+ p \quad \text{or} \quad \rho^+ \pi^0 p \tag{3.1}$$

(or the analogous π^--initiated reactions) and a spin-parity analysis for the ρ-π subsystem are described in this section. Experimentally, data are only available on the ρ^0 final state. In particular we are interested in the A mass region

$$0.9 \leq (s_1)^{1/2} \leq 1.5 \text{ GeV}$$

for small squared momentum transfers t_2 to the proton.

At high total invariant energy squared s the double-Regge graphs shown in Fig. 4 can contribute to the reactions (3.1). Double baryon exchange is improbable and therefore has been omitted. In the Dalitz plot the graphs of Fig. 4 contribute as shown in Fig. 5. Only the graphs in Figs. 4(a), 4(b), and 4(b′) are of interest to us because only these contribute significantly at small invariant energies squared s_1 of the subsystem.

We use the high-energy form of the double-Regge amplitude and do not discuss here the complicated question of kinematic singularities[19] and nonasymptotic corrections. Also we shall assume that the dependence of the middle vertex $\gamma_{\lambda_2}(t_1, t_2, \omega)$ on the angle ω may be neglected.

Pion exchange dominates the ρ-π subsystem at small momentum transfer squared t_1 to the ρ meson and corresponds to helicity $\lambda_1 = 0$ in the s_1 brick-wall frame (i.e., the sense-sense amplitude at the physical pion-exchange pole). Indeed, experimentally the ρ meson is produced strongly aligned with a spin state $M = 0$ along the beam in the ρ rest frame. As in quasi-two-body processes, observed deviations of the spin density matrix from the value $\rho_{00} = 1$ indicate the presence of other amplitudes. For values of $|t_1| = 0.2$ GeV^2 to 1 GeV^2, A_2 exchange may be quite important. Also, graphs of the type where the ρ meson is produced at the middle vertex [see Figs. 4(b), 4(b′)] will contribute when s_1 is small. In fitting the data these contributions should not in general be neglected, particularly since the t_1 squared-momentum-transfer distributions in many-body processes are much broader than in two-body processes (mainly due to phase-space differences[7]).

For graphs of the type where the pion is produced at the middle vertex [see Fig. 4(a)], the assumption that the amplitude is an even function of $\sin\omega$ requires [see Eq. (2.15)] that the normalities of the trajectories α_1 and α_2 be opposite.[27] To

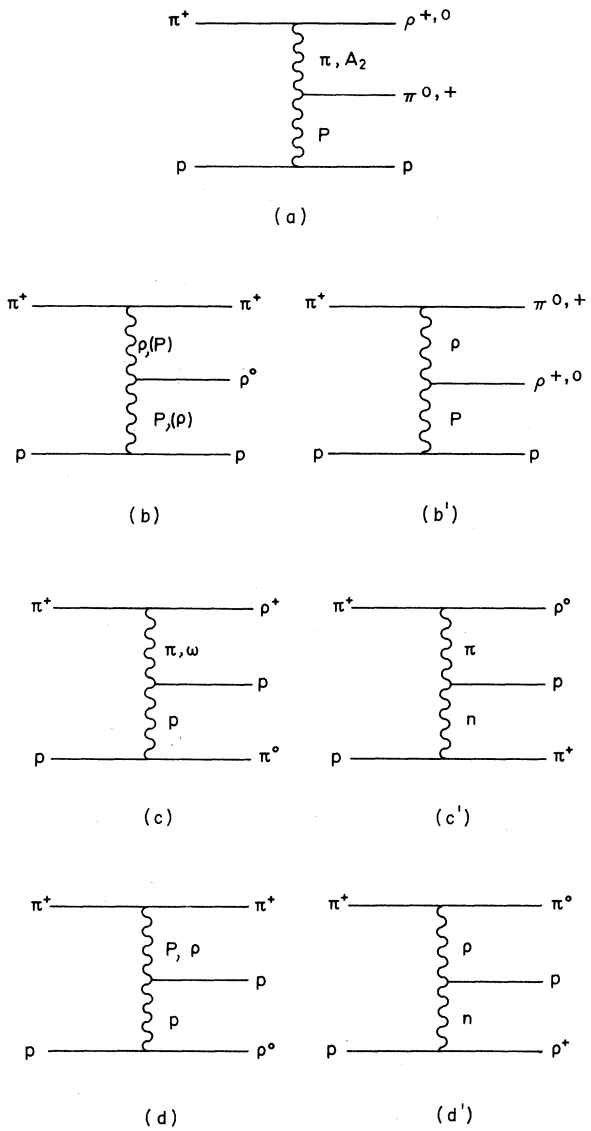

FIG. 4. Double-Regge-pole exchange diagrams which contribute to the reaction $\pi p \to \rho \pi p$.

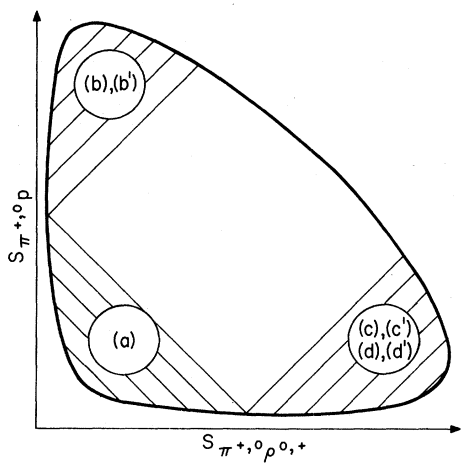

FIG. 5. Regions of the Dalitz plot where the graphs in Fig. 4 are expected to contribute.

populate states with $\bar{\lambda}_1 = 0$, we require the trajectory α_1 to have unnatural parity. For the amplitudes with $\bar{\lambda}_1 = \pm 1$, α_1 can have either normality. In the case of type 4(b), 4(b′) graphs, the trajectory α_1 must have natural parity to obtain a nonzero coupling to two pions. The "middle" particle is now the ρ meson and, for $\lambda_2 = 0$, we require the trajectories α_1 and α_2 to have the same normality.

We have little information on the magnitude and phase [and helicity structure for type 4(b), 4(b′) graphs] of the other double-Regge graphs relative to the pion-exchange process. To illustrate our method we confine ourselves to the traditional pion-exchange (Reggeized Deck) term, which is dominant at small t_1, combined with diffraction scattering. In fact, Berger[2] has obtained a good average fit to data at 8 (Ref. 28), 13, and 20 (Ref. 29) GeV/c in a wide range of s_1 values around the A mass enhancement, with a Reggeized pion ($\alpha_1 = \alpha_\pi$) and an effectively flat Pomeranchon ($\alpha_2 = \alpha_P$) exchanged [see Fig. 4(a)]. The amplitude used is

$$f_{\bar{\lambda}_1=0}(s, s_1, s_2, t_1, t_2) = [1+\exp(-i\pi\alpha_\pi)][1+\alpha_\pi(t_1)]\left(\frac{s_1 - t_2 - m_\pi^2 - (m_\rho^2 - m_\pi^2 - t_1)(t_2 + t_1 - m_\pi^2)/2t_1}{s_0}\right)^{\alpha_\pi} \frac{\exp(\frac{1}{2}at_2)[\lambda(s_2, m_N^2, m_\pi^2)]^{1/2}}{\sin\pi\alpha_\pi(t_1)} . \tag{3.2}$$

It has no explicit dependence on $\sin\omega$, and we have introduced the Regge signature factor[14,15,20] for the pion trajectory $\alpha_\pi(t_1)$ in the t_1 channel. Here $s_0 = 1$ GeV^2 and $a = 8$ GeV^{-2} at $P_{\text{lab}} = 8$ GeV/c. Dependence on the nucleon helicities $\bar{\mu}_b$ and μ_3, which is factorizable and mainly nonflip for small t_2, has been omitted.

For small t_1 values a linear pion trajectory (i)

$$\alpha_\pi(t_1) = (t_1 - m_\pi^2)\alpha_\pi' , \tag{3.3}$$

with a slope $\alpha_\pi' = 1$ GeV^{-2}, and a curved trajectory of the Pignotti type (ii)

$$\alpha_\pi(t_1) = (t_1 - m_\pi^2)(m_\pi^2 - t_1 + 1)^{-1} \tag{3.4}$$

give similar results.[2] With the linear trajectory (i), the Berger amplitude (3.2) develops "ghosts" at $\alpha_\pi(t_1) = -2, -3, -4$, etc. However, pion exchange is only expected to be dominant for small t_1 and, following Berger,[2] a cutoff is applied for large values of $|t_1|$ (i.e., $|t_1| > 0.97$ GeV^2) when using trajectory (i). Differences introduced between the results of our spin-parity analysis for trajectories (i) and (ii), respectively, due to different behavior at larger $|t_1|$ values, gives some indication of the uncertainty involved in this simple Reggeized Deck model of the process $\pi N \to \rho\pi N$. It should be remarked that the double-Regge amplitude is not determined by a direct fit to the region of the Dalitz plot where all the final-state two-particle subenergies are relatively large, but is essentially chosen to fit the events with $s_1 \leq 2.5$ GeV$^2 \leq s_2$. However, for small t_1, the Reggeized pion is not far off the mass shell, and the double-Regge parameters are reasonably well fixed by the ρ decay width and πN elastic scattering (as in the original Deck model). Including other exchanges, such as P' and ρ, in the t_2 channel, in addition to the Pomeranchon, will alter the dynamical dependence on s_2 at subasymptotic energies. Here we follow Berger and neglect such effects. It should also be pointed out that the phase of the amplitude has not been tested at all experimentally.

Inserting the amplitude (3.2) into Eq. (2.19) and using Eqs. (2.28)–(2.29), we find the ρ-π helicity partial waves of definite normality N, which we abbreviate as $a_{\lambda_1}^{JM,N}(s, s_1, t_2)$, in the ρ-π Jackson frame. For $\lambda_1 = 0$ only states of abnormal parity $N = (-1)^J P = -1$ can be formed, whereas for $\lambda_1 = 1$ both parities can contribute. Explicitly, we have

$$a_{\lambda_1=0}^{JM-}(s, s_1, t_2) = \left(\frac{2J+1}{\pi}\right)^{1/2} \int_{t_1^{\min}}^{t_1^{\max}} dt_1 \int_{s_2^{\min}}^{s_2^{\max}} ds_2 J(s, s_1, s_2, t_1, t_2) \cos M\phi\, d_{M0}^J(\theta) d_{00}^1(\chi_1) f_{\bar{\lambda}_1=0}(s, s_1, s_2, t_1, t_2) \tag{3.5}$$

and

$$a_{\lambda_1=1}^{JM\pm}(s, s_1, t_2) = \left(\frac{2J+1}{2\pi}\right)^{1/2} \int_{t_1^{\min}}^{t_1^{\max}} dt_1 \int_{s_2^{\min}}^{s_2^{\max}} ds_2 J(s, s_1, s_2, t_1, t_2) \cos M\phi [d_{M1}^J(\theta) \pm d_{M-1}^J(\theta)] d_{10}^1(\chi_1) f_{\bar{\lambda}_1=0}(s, s_1, s_2, t_1, t_2). \tag{3.6}$$

It follows from Eq. (2.32) that

$$a_{\lambda_1}^{JM\pm}(s, s_1, t_2) = \mp (-1)^M a_{\lambda_1}^{J-M\pm}(s, s_1, t_2). \tag{3.7}$$

The partial waves $A_L^{JM}(s, s_1, t_2)$ of definite orbital angular momentum L, with $L=J\pm1$ for abnormal-parity and $L=J$ for normal-parity states, are given by[21]

$$A_{L=J-1}^{JM} = \left(\frac{J+1}{2J+1}\right)^{1/2} a_1^{JM-} + \left(\frac{J}{2J+1}\right)^{1/2} a_0^{JM-}, \tag{3.8}$$

$$A_{L=J+1}^{JM} = \left(\frac{J}{2J+1}\right)^{1/2} a_1^{JM-} - \left(\frac{J+1}{2J+1}\right)^{1/2} a_0^{JM-}, \tag{3.9}$$

$$A_{L=J}^{JM} = a_1^{JM+}. \tag{3.10}$$

The partial waves have been evaluated numerically, for $s=15.9$ GeV^2 ($P_{\text{lab}}=8$ GeV/c) and $t_2=-0.1$ GeV^2, at various values of s_1 in the region of the A mass enhancement. The percentage contributions of the partial waves $A_L^{JM}(s, s_1, t_2)$ to the cross section $\partial^2\sigma/\partial t_2 \partial s_1$ are given in Table I for both trajectories (i) and (ii), at invariant ρ-π subenergies squared $s_1=0.85$, 1.15, and 1.65 GeV^2. In Figs. 6 and 7, we plot the real and imaginary parts of the important helicity partial waves $a_{\lambda_1}^{JM,N}(s, s_1, t_2)$ for trajectories (i) (continuous line) and (ii) (broken line) as a function of s_1. Along the curves, the s_1 variation is marked in steps of $s_1=0.1$ GeV^2, from $s_1=0.85$ GeV^2 to 2.45 GeV^2 (i.e., $m_{\rho\pi}$ from threshold up to 1.56 GeV). The sizeable $L=J-1$ orbital angular momentum amplitudes A_L^{JM} with $J=1$ and 2 are shown in Fig. 8. We have also plotted Argand diagrams of the quantities $(q_{\rho\pi})^{L+1}A_L^{JM}$ in Fig. 9, for the important partial waves. This procedure is only meaningful at small values of s_1, where $(q_{\rho\pi})^{L+1}A_L^{JM}$ has the same threshold behavior $(q_{\rho\pi})^{2L+1}$ as the corresponding elastic ρ-π phase shift, but it is not, of course, bounded by the unitarity circle familiar in elastic scattering phase-shift analysis.

TABLE I. The percentage contributions of the partial-wave amplitudes $A_L^{JM}(s, s_1, t_2)$ to the cross section (2.33) obtained with the trajectories (i) and (ii) for $P_{\text{lab}}=8$ GeV/c, $t_2=-0.1$ GeV^2, and $s_1=0.85$, 1.15, and 1.65 GeV^2.

$\lvert A_L^{JM}\rvert^2$ \ s_1 (GeV^2)	0.85		1.15		1.65	
	(i)	(ii)	(i)	(ii)	(i)	(ii)
$\lvert A_P^{00}\rvert^2$	0.5	0.7	2.8	5.0	1.9	9.9
$\lvert A_S^{10}\rvert^2$	93.6	93.8	74.3	80.4	37.4	69.5
$\lvert A_D^{10}\rvert^2$	<0.1	<0.1	<0.1	<0.1	1.7	<0.1
$2\lvert A_S^{11}\rvert^2$	<0.1	<0.1	0.3	0.2	0.6	0.6
$2\lvert A_D^{11}\rvert^2$	<0.1	<0.1	0.2	<0.1	0.6	<0.1
$\lvert A_P^{10}\rvert^2$	0.0	0.0	0.0	0.0	0.0	0.0
$2\lvert A_P^{11}\rvert^2$	1.1	1.1	4.3	4.0	4.1	3.8
$\lvert A_P^{20}\rvert^2$	0.3	0.1	8.3	1.9	30.9	6.0
$\lvert A_F^{20}\rvert^2$	<0.1	<0.1	<0.1	<0.1	<0.1	<0.1
$2\lvert A_P^{21}\rvert^2$	1.1	1.1	3.1	3.2	1.3	2.0
$2\lvert A_F^{21}\rvert^2$	<0.1	<0.1	<0.1	<0.1	0.2	<0.1
$2\lvert A_P^{22}\rvert^2$	<0.1	<0.1	<0.1	<0.1	<0.1	<0.1
$2\lvert A_F^{22}\rvert^2$	<0.1	<0.1	<0.1	<0.1	<0.1	<0.1
$\lvert A_D^{20}\rvert^2$	0.0	0.0	0.0	0.0	0.0	0.0
$2\lvert A_D^{21}\rvert^2$	<0.1	<0.1	0.6	0.3	1.9	0.7
$2\lvert A_D^{22}\rvert^2$	0.1	0.1	<0.1	0.1	<0.1	<0.1
$J>2$	3.2	3.0	6.0	4.8	19.3	7.4

IV. DISCUSSION AND CONCLUSIONS

Here we discuss the results obtained in the previous section. The Deck effect,[1] or elementary one-pion-exchange diffraction scattering, has been known for some time to give an enhancement at small s_1 for the reaction (3.1). Berger[2] has shown that the Reggeized-pion version of this model leads to a substantial decrease in the calculated width of the low-mass ρ-π enhancement. The predicted peak position of 1100 MeV and width of 350 MeV are fairly independent of the incident pion energy. This model reproduces quite well the shape, including the position of the A_1 peak, of the whole A enhancement[28,29] apart from the A_2 peak at lower incident pion energies. Empirically, Pomeranchon exchange does not appear to contribute at all to such processes,[30] and we should therefore not expect the A_2 to be contained in the Reggeized Deck amplitude. However, the question of the energy dependence of A_1 and A_2 production has yet to be settled definitely.[31,32] Clearly, careful partial-wave analyses of the 3π production data[33] at various energies are required. Also a study of the $K\bar{K}$ decay mode of the A_2 resonance will not suffer from the large diffractive production of unnatural-parity ρ-π states.

Though its predictions of the various angular correlations have not been tested in detail, the Berger amplitude reproduces the available experimental distributions quite well.[34] In particular it gives nonisotropic Treiman-Yang angular distributions, in contrast to the elementary one-pion-exchange model.[2,29] The absolute normalization of the cross section predicted by the Reggeized Deck amplitude is about 30% smaller than that observed experimentally. There also appears to be some backward-forward asymmetry in the decay of the ρ^0, indicating the presence of a scalar π-π background,[28,33,35,36] possibly associated with an A_1

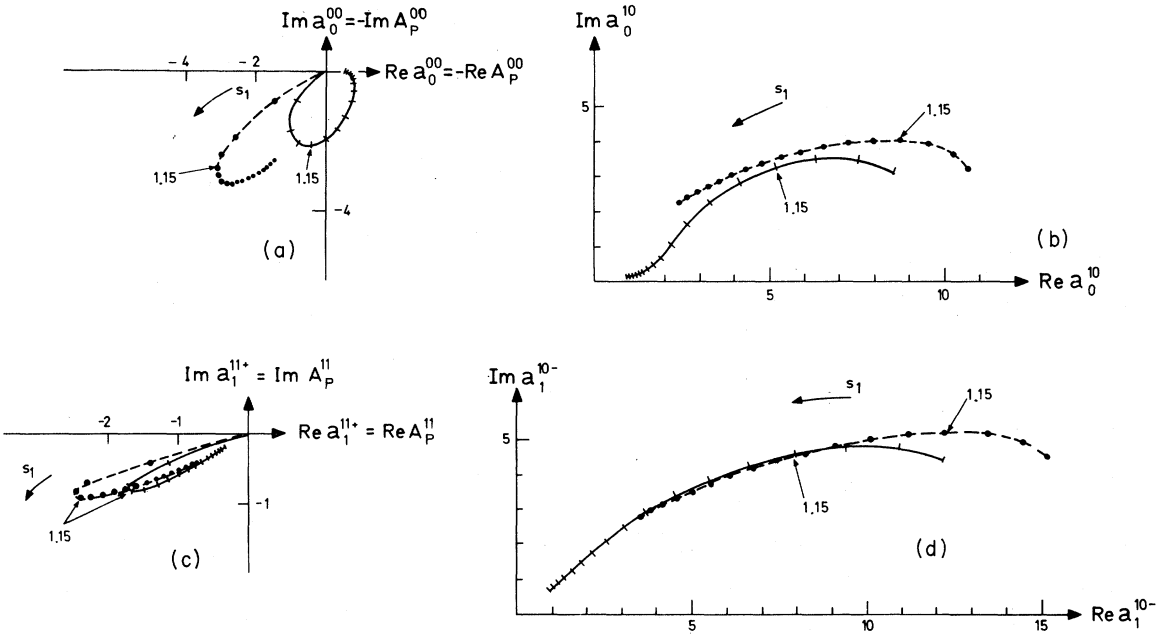

FIG. 6. Argand diagrams of the important helicity partial-wave amplitudes $a_{\lambda_1}^{JM,N}(s,s_1,t_2)$ with $J=0$ and $J=1$, at $P_{\text{lab}}=8$ GeV/c and $t_2=-0.1$ GeV^2, in arbitrary units. The continuous (broken) line corresponds to the straight-line trajectory (i) [Pignotti trajectory (ii)]. Along the curves the s_1 variation is marked in steps of $s_1=0.1$ GeV^2 from 0.85 GeV^2 to 2.45 GeV^2. The position of the A_1 peak at $s_1=1.15$ GeV^2 ($m_{3\pi}=1.07$ GeV) is marked with an arrow.

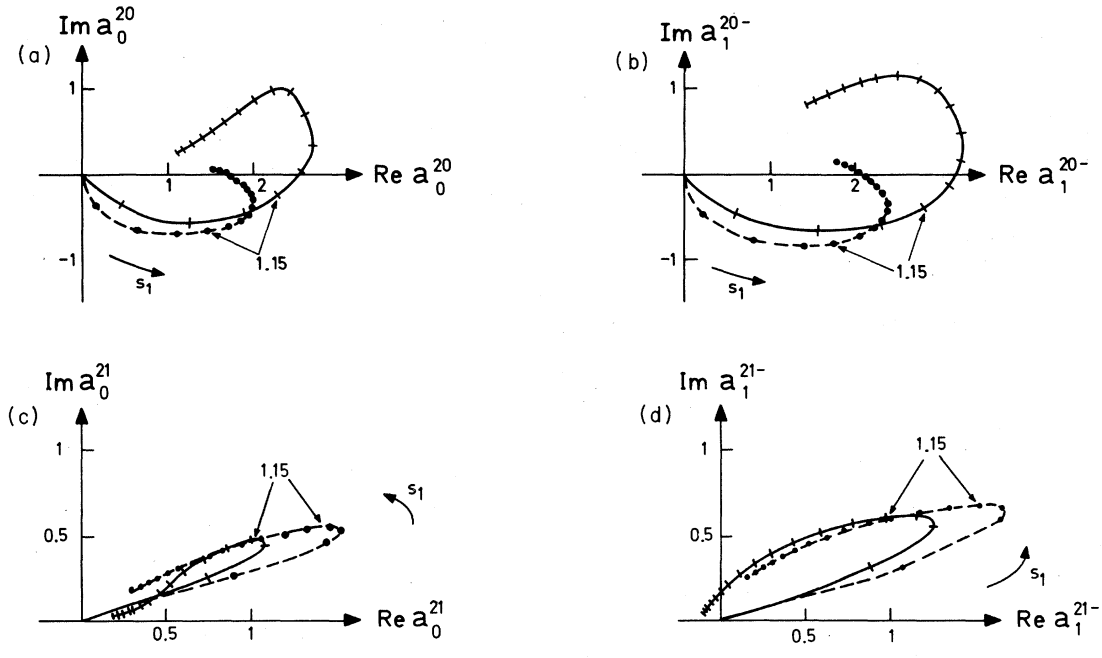

FIG. 7. Argand diagrams of the important $J=2$ helicity partial-wave amplitudes with the same notation as in Fig. 6.

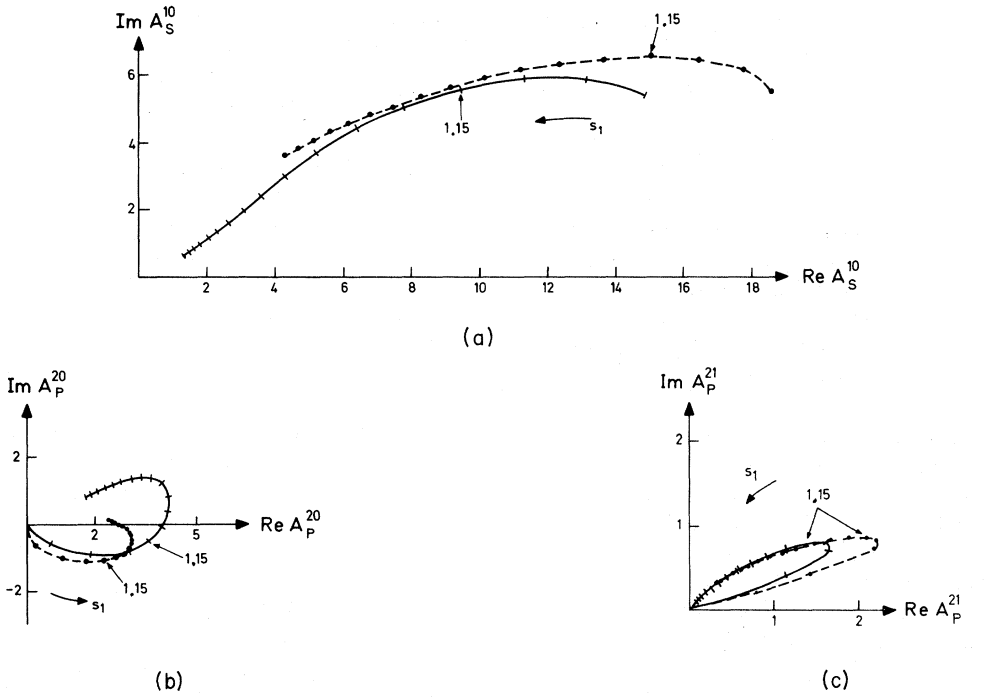

FIG. 8. Argand diagrams of the sizeable orbital angular momentum partial-wave amplitudes $A_L^{JM}(s, s_1, t_2)$ using the same notation as in Fig. 6.

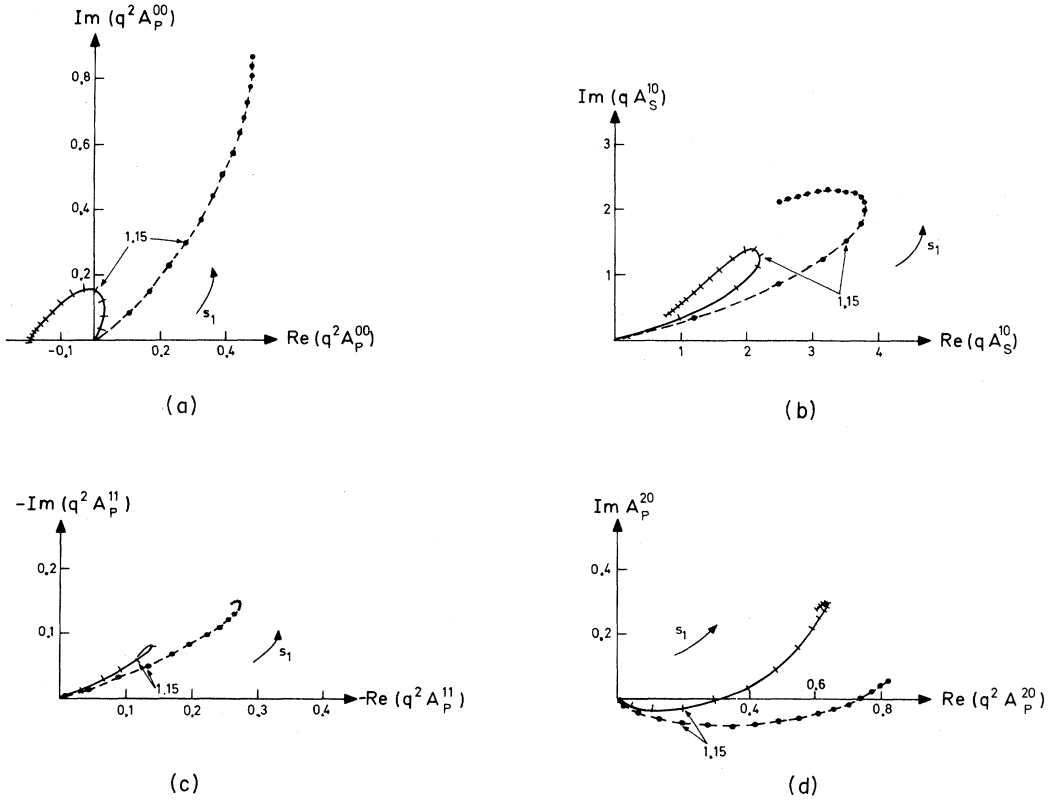

FIG. 9. Argand diagrams of the important orbital angular momentum partial-wave amplitudes $A_L^{JM}(s, s_1, t_2)$ multiplied by the threshold factor $(q_{\rho\pi})^{L+1}$, using the same notation as in Fig. 6.

daughter state,[28] with $J^P = 0^-$ and decaying into ϵ-π. The application of the double-Regge model at subasymptotic energies has been quite successful for a number of one-pion-exchange diffractive scattering reactions.[2,12,37] Chew and Pignotti[4] have suggested that the duality[3,38,39] between t-channel and s-channel processes might justify this success, and that the double-Regge model should give a reasonably good semilocal average description of the data at all subenergies. In these three-body applications it is necessary to use $|f_{\lambda_i}|^2$ and not simply the absorptive part of the amplitude $\mathrm{Im}f_{\lambda_i}$. Application of duality to the full amplitude in two-body reactions is sometimes, but by no means always, successful.[39,40] Evidence for Reggeization of the pion is difficult to establish from two-body data, where absorptive corrections often appear to be important and the energy dependence is similar to elementary pion exchange. The low mass of the pion causes a nearby pole in the momentum transfer squared t_1 and is therefore "peripheral" at all energies. This is the situation where the use of the Regge representation at low s_1 has the most chance of success. Although the use of the double-Regge amplitude (3.2) cannot be entirely justified from our experience with two-body amplitudes, it has so far given good agreement with data and is probably quite reasonable at small t_1 values.

There has been much discussion as to whether the A_1 should be considered a resonance, generally classified[41,42] as the isovector member of an axial-vector nonet with $J^{PC} = 1^{++}$, or purely a kinematic effect. A variety of theoretical predictions[43,44] for the properties of an A_1 resonance is given in the literature. In some papers, S-wave and D-wave A_1 couplings are interpreted as nonderivative and derivative couplings, respectively. For pure S-wave coupling, this identification is almost exact. The general connection of the usual orbital angular momentum notation of Eqs. (3.6)–(3.8), for $J = 1$, with the tensor couplings[43]

$$\mathfrak{M} = A\epsilon^{\rho}\cdot\epsilon^{A_1} - B\epsilon^{A_1}\cdot P_{\rho}\epsilon^{\rho}\cdot P_{A_1}\ , \tag{4.1}$$

is given by

$$a_1^{1M-} = g_M[\sqrt{2}\,A], \tag{4.2}$$

$$a_0^{1M-} = g_M[(E_\rho/m_\rho)A - \vec{\mathrm{p}}_\rho{}^2(m_{A_1}/m_\rho)B]. \tag{4.3}$$

Here g_M is the production amplitude for the 1^+ particle having spin component M, and $P_\rho = (E_\rho, \vec{\mathrm{p}}_\rho)$ is referred to the A_1 rest frame.

The experimental situation[28,29,33,42,45,46] is somewhat complicated. The ρ-π states produced in the A_1 mass region have usually been interpreted as mainly 1^+ S-wave states, having spin component $M = 0$ along the beam direction, but the presence of significant amounts of D-wave or 2^- states has been reported.[46] However, recent sophisticated data analyses[33] indicate the 1^+ component of the A bump to be almost pure S-wave. There is some evidence for neutral A_1 production,[42,47] which appears not to be adequately explained by a simple charge-exchange Deck effect. On the other hand a recent study of the reaction $\pi^- n \to \pi^-\pi^- p$, where the meson system has isospin 2, finds consistency with the charge-exchange Deck effect.[48] A_1 production has been reported in processes where the usual Deck mechanism cannot contribute,[42,49] but as yet the evidence for nondiffractive A_1 production is not compelling.[50]

Chew and Pignotti[4] have interpreted the low-invariant-mass ρ-π enhancement required by the Reggeized Deck amplitude as a prediction of the existence of an A_1 resonance. However, pion exchange gives a predominantly real (i.e., nonabsorptive) amplitude in the s_1 variable, while an A_1 resonance would give a mainly imaginary amplitude. Thus the interpretation, in a finite-energy sum-rule sense, of the Reggeized Deck amplitude as resonance-dominated at the A_1 mass is invalid. We will now use the results of Sec. III to compare the spin-parity content of the Berger amplitude with that expected for a resonating A_1 meson.

As can be seen in Table I, the results for both trajectories are similar from threshold up to the A_1 mass and, in the ρ-π Jackson frame, the A_S^{10} partial wave is dominant. At the A_1 mass, $s_1 = 1.15$ GeV^2, 75–80% of the cross section is due to this $J^P = 1^+$ S-wave state with $M = 0$, in agreement with previous estimates.[2,35] The regions of (s_2, t_1) phase space which contribute are shown in Figs. 10(a) and 10(b), for $s_1 = 0.9$ and 1.1 GeV^2, respectively. The assumption of pion-exchange dominance in the t_1 channel does not seem too unreasonable in these regions,[51] though it becomes less justified for larger t_2 values, or for values of s_1 above the A_1 mass. Nondiffractive πN scattering could contribute quite significantly for $P_{\mathrm{lab}} = 8$ GeV/c and provide some non-S-wave states, which would go away as the incident momentum increased. The Berger amplitude analyzed here only includes Pomeranchon exchange, which is expected to persist at all momenta. The nonvanishing $M \neq 0$ partial waves are due to the Reggeization of the pion and reflect the nonisotropic Treiman-Yang distributions. We remark here that the amplitudes A_L^{JM}, for production of ρ-π states with definite J and L, still almost conserve t_2-channel helicity and definitely violate s-channel helicity conservation.[32,52]

Dominance of the cross section by a $J^P = 1^+$ ρ-π state is clearly consistent with an averaged de-

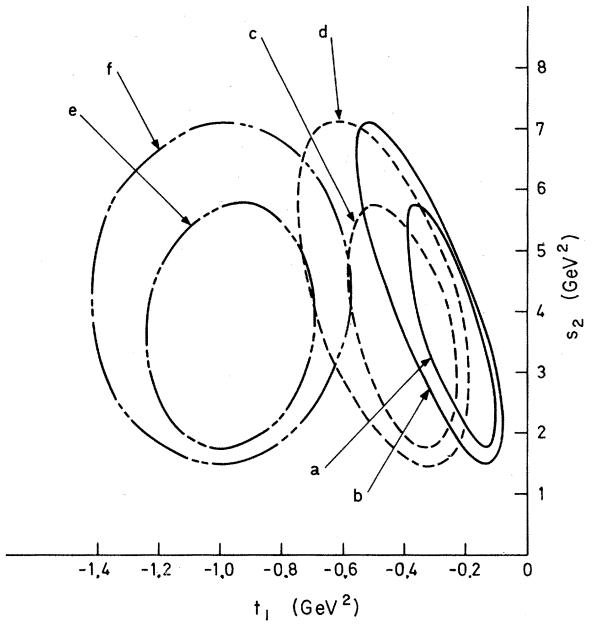

(a) $s_1 = 0.95$ GeV^2, $t_2 = -0.1$ GeV^2
(b) $s_1 = 1.1$ GeV^2, $t_2 = -0.1$ GeV^2
(c) $s_1 = 0.95$ GeV^2, $t_2 = -0.3$ GeV^2
(d) $s_1 = 1.1$ GeV^2, $t_2 = -0.3$ GeV^2
(e) $s_1 = 0.95$ GeV^2, $t_2 = -1.0$ GeV^2
(f) $s_1 = 1.1$ GeV^2, $t_2 = -1.0$ GeV^2

FIG. 10. Phase-space boundaries in (s_2, t_1) for different values of (s_1, t_2) at $P_{\text{lab}} = 8$ GeV/c for the reaction $\pi p \to \rho\pi p$.

scription of A_1 resonance production. Since no appreciable D-wave or $M \neq 0$ amplitudes are present, it is not possible to make a practical test of the factorization property required by resonance production, mentioned at the end of Sec. II and embodied in Eqs. (4.2) and (4.3). Hence the only way to distinguish between the Reggeized Deck amplitude and dominant A_1 resonance production is by studying the relative phases of the various partial waves and their s_1 dependence.

We now consider the s_1 dependence of the ρ-π partial-wave states, with $J \leq 2$, which contribute significantly between threshold and 2.5 GeV^2. In Figs. 6–8, we show Argand diagrams of the important helicity and orbital partial waves. Due to the closeness of the pion pole at $t_1 = m_\pi^2$, the Reggeized Deck amplitude falls off very rapidly with increasing t_1 and the partial-wave integrations are weighted at small t_1. So, the resulting phase variation with s_1 is not strong, and the partial waves do not show fully developed Schmid loops[39] corresponding to a linearly rising trajectory of resonances in the ρ-π channel. Introducing the threshold factor $(q_{\rho\pi})^{L+1}$, as in Fig. 9, gives extra structure in the partial waves A_L^M, but an interpretation of the resulting curvature in terms of resonant behavior, with appreciable inelasticity and background, is not convincing. In particular, there is no evidence for local resonant behavior in the dominant A_S^{10} wave at the A_1 mass.

Phenomenologically it is very difficult to determine the phase variation of the S-wave ρ-π amplitude at the A_1 mass, since there is no other important amplitude present to provide a reference phase. The only other appreciable amplitude seems[33] to come from the S-wave decay of the $J^P = 0^-$ 3π state into ϵ-π, which is responsible for the backward-forward asymmetry mentioned earlier. However, there might be an A_1 daughter state causing this amplitude to resonate also.

Although a detailed partial-wave analysis has not yet solved the puzzle of the A_1, it has been very successful[33] in studying the 2^+ partial wave at the A_2 mass, for incident beam momenta below 10 GeV/c. The s_1 dependence of the magnitude and phase of the partial wave clearly shows the existence of an A_2 resonance. It is of some interest to extend this analysis to higher beam momenta in order to determine the s dependence of A_2 production[30,31], as seen via its ρ-π decay mode. A similar careful analysis is required, since there is a large diffractive ρ-π background in other spin-parity states. We have given the partial-wave decompositions of the Berger amplitude at the A_2 mass, $m_{\rho\pi} = 1.3$ GeV, to indicate the ρ-π states, which might be diffractively produced in this region.

The region of integration increases with s_1, and different amplitudes A_L^M are obtained with the trajectories (i) and (ii). The partial wave A_P^{20} becomes important for the straight-line trajectory and is equal in magnitude to A_S^{10} at $s_1 = 1.75$ GeV^2 However, in the $A_{1,5}$ region,[42] the S wave still provides over half of the cross section. On the other hand, the Pignotti trajectory causes the A_S^{10} wave to dominate strongly the whole A enhancement, $s_1 \leq 2$ GeV^2, and makes A_P^{00} the next largest amplitude. As expected, all these states have predominantly unnatural parity. The difference in the results, obtained with the two trajectories, reflect the ambiguity in the Deck amplitude and the large effect other exchanges could have as s_1 increases.

In conclusion, it is at present difficult to distinguish, phenomenologically, between the Reggeized Deck amplitude and dominant A_1 resonance production. Dual-resonance models do not solve this problem.[8] It has been suggested that a search for structure in the s_1 dependence of the slope of the t_2 momentum-transfer-squared distribution

could be helpful.[53] Empirically the relative amounts of 0^-, 1^+, 2^-, and 1^- ρ-π partial waves are in reasonable agreement[33] with that predicted by the Reggeized Deck model. There is conflicting evidence regarding the success of the charge-exchange Deck effect.[47,48] The most satisfactory confirmation for the existence of an A_1 resonance would be convincing evidence for A_1 production in some process where the usual Deck mechanism cannot operate.

ACKNOWLEDGMENTS

The authors would like to thank Dr. G. Ringland for provoking this investigation and his interest in it. We are grateful to Professor L. Castillejo for many helpful discussions. We should also like to acknowledge conversations with Dr. E. Berger, Professor G. Chew, Dr. G. Immirzi, Dr. B. Martin, Dr. R. J. N. Phillips, and Dr. C. Wilkin, and correspondence with Dr. G. C. Fox.

APPENDIX

The cosine of the Treiman-Yang angle ϕ (see Fig. 4) is

$$\cos\phi = (\vec{p}_a\times\vec{p}_1)\cdot(\vec{p}_b\times\vec{p}_3)[\,|\vec{p}_a\times\vec{p}_1|\,|\vec{p}_b\times\vec{p}_3|\,]^{-1}|_{\vec{p}_1+\vec{p}_2=0} \tag{A1}$$

$$= N(s, s_1, s_2, t_1, t_2)[D_1(s_1, t_1, t_2)D_2(s, s_1, t_2)]^{-1/2}. \tag{A2}$$

Evaluating the determinants N, D_1, and D_2 we obtain

$$N(s, s_1, s_2, t_1, t_2) = G_2(s, s_1, t_1, t_2) - s_2 G_1(s_1, t_2)\,, \tag{A3}$$

where

$$8G_1(s_1, t_2) = \lambda(s_1, t_2, m_a^2) \tag{A4}$$

and

$$\begin{aligned}8G_2(s, s_1, t_1, t_2) = {} & m_b^2[(s_1 - s)(t_1 - t_2 + s_1 - m_1^2) - m_2^2(s_1 - t_2 + m_a^2) - m_3^2(m_a^2 + m_1^2 - t_1)] \\ & - t_1[(s_1 - s)(t_2 - s_1 + m_a^2) + (m_b^2 - t_2)(t_2 - s_1 - m_a^2) + 2m_a^2 m_3^2] \\ & + (s - m_a^2)[(m_b^2 - t_2)(t_1 - t_2 + s_1 - m_1^2) + m_2^2(s_1 - t_2) + m_3^2(m_1^2 - t_1) - m_a^2(m_2^2 + m_3^2)] \\ & - (t_2 - m_3^2)[(s_1 - s)(m_1^2 - t_1 - m_a^2) + (m_a^2 + m_1^2 - t_1)(m_b^2 - t_2) + 2m_a^2 m_2^2]\,.\end{aligned} \tag{A5}$$

Also, we have

$$\begin{aligned}4D_1(s_1, t_1, t_2) = {} & -t_1^2 s_1 + t_1[2m_1^2 t_2 + m_a^2(s_1 - m_1^2 + m_2^2) + (t_2 - s_1)(s_1 - m_1^2 - m_2^2)] \\ & - m_1^2(s_1 - t_2 - m_1^2)^2 - m_2^2(m_a^2 + m_1^2)^2 - m_a^2(s_1 - m_1^2 - m_2^2)^2 \\ & + (m_a^2 + m_1^2)(s_1 - t_2 - m_1^2)(s_1 - m_1^2 - m_2^2) + 4m_a^2 m_1^2 m_2^2\end{aligned} \tag{A6}$$

and

$$\begin{aligned}4D_2(s, s_1, t_2) = {} & (t_2 - m_b^2 - m_3^2)(s_1 + m_b^2 - t_2 - s)(s - m_a^2 - m_b^2) \\ & - m_3^2(s - m_a^2 - m_b^2)^2 - m_a^2(m_b^2 + m_3^2 - t_2)^2 - m_b^2(m_b^2 + s_1 - s - t_2)^2 + 4m_a^2 m_b^2 m_3^2\,.\end{aligned} \tag{A7}$$

The maximal and minimal values for t_1 can be found from the condition $-1 \leq \cos\theta \leq 1$, where $\cos\theta$ is given in Eq. (2.26). This gives

$$t_1^{\max,\min} = \{\pm[\lambda(s_1, m_a^2, t_2)\lambda(s_1, m_1^2, m_2^2)]^{1/2} - s_1^2 + s_1(t_2 + m_a^2 + m_1^2 + m_2^2) - (m_a^2 - t_2)(m_1^2 - m_2^2)\}/(2s_1)\,. \tag{A8}$$

Note that $t_1^{\max}$ corresponds to $\theta = 0$ and $t_1^{\max} > t_1^{\min}$. Similarly the maximal and minimal values of s_2 can be obtained from Eq. (A2) and the condition $-1 \leq \cos\phi \leq 1$, which gives

$$s_2^{\max,\min} = \{\pm[D_1(s_1, t_1, t_2)D_2(s, s_1, t_2)]^{1/2} + G_2(s, s_1, t_1, t_2)\}/G_1(s_1, t_2)\,. \tag{A9}$$

Figure 10 shows the integration region in Eqs. (2.28)–(2.29) for a few values of the parameters s, s_1, and t_2 for the reaction $\pi N \to \rho\pi N$.

The Jacobian in the integrand of Eq. (2.30) is

$$J(s, s_1, s_2, t_1, t_2) = \partial(\cos\theta, \phi)/\partial(s_2, t_1) = \tfrac{1}{2} s_1 [\lambda(s_1, m_1^2, m_2^2)(-\Delta_4)]^{-1/2}, \quad \text{(A10)}$$

where the Gram determinant Δ_4 is given by

$$(-\Delta_4) = 4(D_1 D_2 - N^2)/\lambda(s_1, m_a^2, t_2). \quad \text{(A11)}$$

The function $\lambda(x, y, z)$ is defined in Eq. (2.5).

---

*Much of this work was done while visiting University College, London, and supported in part by the Science Research Council.

†Royal Society European Research Fellow.

[1]R. T. Deck, Phys. Rev. Letters 13, 169 (1964).

[2]E. Berger, Phys. Rev. 166, 1525 (1968); 179, 1567 (1969).

[3]R. Dolen, D. Horn, and C. Schmid, Phys. Rev. 166, 1768 (1968).

[4]C. F. Chew and A. Pignotti, Phys. Rev. Letters 20, 1078 (1968).

[5]P. H. Frampton, K. Schilling, and C. Schmid, Phys. Letters 36B, 361 (1971).

[6]C. D. Froggatt and G. Ranft, Phys. Rev. Letters 23, 943 (1969).

[7]Chan Hong-Mo *et al.*, Nucl. Phys. B19, 173 (1970); A. J. Wroblewski, in *Proceedings of the Fifteenth International Conference on High Energy Physics, Kiev, U.S.S.R., 1970* (Atomizdat, Moscow, 1971).

[8]E. Berger, in *Phenomenology in Particle Physics, 1971,* edited by C. B. Chiu *et al.* (California Institute of Technology, Pasadena, 1971).

[9]Chan Hong-Mo, J. Łoskiewicz, and W. W. M. Allison, Nuovo Cimento 57A, 93 (1968); E. Plahte and R. G. Roberts, Lett. Nuovo Cimento 1, 187 (1969); J. Bartsch *et al.*, Nucl. Phys. B19, 381 (1970); S. Humble, Nucl. Phys. B28, 416 (1971).

[10]C. F. Chew and A. Pignotti, Phys. Rev. 176, 2112 (1968); C. F. Chew, M. L. Goldberger, and F. Low, Phys. Rev. Letters 22, 208 (1969); L. Caneschi and A. Pignotti, Phys. Rev. Letters 22, 1219 (1969).

[11]I. G. Halliday, Nuovo Cimento 60A, 177 (1969); Nucl. Phys. B21, 445 (1970).

[12]J. D. Jackson, in *Proceedings of the Lund International Conference on Elementary Particles,* edited by G. von Dardel (Berlingska Boktryckeriet, Lund, Sweden, 1970).

[13]K. Gottfried and J. D. Jackson, Nuovo Cimento 33, 309 (1964).

[14]N. F. Bali, C. F. Chew and A. Pignotti, Phys. Rev. 163, 1572 (1967).

[15]T. W. B. Kibble, Phys. Rev. 131, 2282 (1963); Chan Hong-Mo, K. Kajantie, and G. Ranft, Nuovo Cimento 49, 157 (1967).

[16]J. F. Boyce, J. Math. Phys. 8, 675 (1967); J. Bjørneboe and Z. Koba, Nucl. Phys. B7, 53 (1968); Z. Koba, Nucl. Phys. B8, 351 (1968).

[17]G. C. Wick, Ann. Phys. (N.Y.) 18, 65 (1962).

[18]T. L. Trueman and G. C. Wick, Ann. Phys. (N.Y.) 26, 322 (1964); G. Cohen-Tannoudji, A. Morel, and H. Navelet, Ann. Phys. (N.Y.) 46, 239 (1968); G. C. Fox, Cambridge University Ph.D. thesis, 1967 (unpublished); C. Quigg, University of California Ph.D. thesis, LRL Report No. UCRL-20032, 1970 (unpublished).

[19]B. E. Y. Svensson, Phys. Rev. 188, 2254 (1969); Nucl. Phys. B15, 93 (1970); G. Cozensa and A. Sciarrino, Nuovo Cimento 68A, 11 (1970); H. Navelet and E. Pittet, Nuovo Cimento 7A, 185 (1972).

[20]See, however, I. T. Drummond, P. V. Landshoff, and W. J. Zakrzewski, Phys. Letters 28B, 676 (1969).

[21]M. Jacob and G. C. Wick, Ann. Phys. 7, 404 (1959).

[22]S. B. Treiman and C. N. Yang, Phys. Rev. Letters 8, 140 (1962).

[23]M. Gell-Mann, M. Goldberger, F. Low, E. Marx, and F. Zachariasen, Phys. Rev. 133, B145 (1964).

[24]In fact for particles 1 and 2 both helicity states (λ_1,λ_2) and $(-\lambda_1,-\lambda_2)$ are included in Eq. (2.33).

[25]K. Watson, Phys. Rev. 88, 1163 (1962); J. S. Ball, W. R. Frazer, and M. Nauenberg, Phys. Rev. 128, 478 (1962).

[26]J. D. Jackson, Nuovo Cimento 34, 1644 (1964).

[27]J. M. Kosterlitz, Nucl. Phys. B9, 273 (1969).

[28]A. M. Cnops *et al.*, Phys. Rev. Letters 21, 1609 (1968); Phys. Letters 29B, 45 (1969).

[29]M. L. Ioffredo *et al.*, Phys. Rev. Letters 21, 1212 (1968).

[30]D. R. O. Morrison, Phys. Letters 25B, 238 (1967); Phys. Rev. 165, 1699 (1968).

[31]K. Paler, Nucl. Phys. B18, 211 (1970); R. G. Roberts, Phys. Letters 35B, 525 (1971); P. G. O. Freund, H. F. Jones, and R. J. Rivers, Phys. Letters 36B, 89 (1971); W. Kittel, CERN Report No. D.Ph. II/Phys. 71-28 (unpublished); T. Ferbel, University of Rochester Report No. UR-875-337.

[32]G. Ascoli *et al.*, Phys. Rev. Letters 26, 929 (1971).

[33]G. Ascoli *et al.*, Phys. Rev. Letters 25, 962 (1970); D. V. Brockway, University of Illinois Report No. COO-1195-197.

[34]See, however, G. W. Brandenburg *et al.*, Nucl. Phys. B16, 287 (1970); and J. W. Lamsa *et al.*, Phys. Rev. D 1, 3091 (1970), who include a ρ-Pomeranchon graph of the type shown in Figs. 4(b) and 4(b′).

[35]J. F. Allard *et al.*, Nuovo Cimento 46A, 737 (1966).

[36]B. J. Deery *et al.*, Phys. Letters 31B, 82 (1970).

[37]J. Andrews *et al.*, Phys. Rev. Letters 22, 731 (1969).

[38]M. Jacob, in *Proceedings of the Lund International Conference on Elementary Particles* (Ref. 12).

[39]C. Schmid, Phys. Rev. Letters 20, 689 (1968); Nuovo Cimento 61A, 289 (1969); Proc. Roy. Soc. (London) A318, 257 (1970).

[40]G. C. Fox, in *High Energy Collisions,* Third International Conference held at State University of New York, Stony Brook, 1969, edited by C. N. Yang *et al.* (Gordon and Breach, New York, 1969).

[41]R. H. Dalitz, in *Proceedings of the Thirteenth International Conference on High Energy Physics, Berkeley, 1966* (Univ. of California Press, Berkeley, 1967); *Symmetry and Quark Models,* edited by R. Chand (Gordon and Breach, New York, 1970).

[42]I. Butterworth, in *Proceedings of the International Conference on Elementary Particles, Heidelberg, Germany, 1967,* edited by H. Filthuth (North-Holland, Am-

sterdam, 1968); Ann. Rev. Nucl. Sci. 19 (1969); B. French, in *Proceedings of the Fourteenth International Conference on High Energy Physics, Vienna, Austria, 1968*, edited by J. Prentki and J. Steinberger (CERN, Geneva, Switzerland, 1968); B. Maglic, in *Proceedings of the Lund International Conference on Elementary Particles* (Ref. 12).

[43]S. Weinberg, in *Proceedings of the Fourteenth International Conference on High Energy Physics, Vienna, Austria, 1968* (Ref. 42); B. Renner, in *Proceedings of the Lund International Conference on Elementary Particles* (Ref. 12); S. Gasiorowicz and D. A. Geffen, Rev. Mod. Phys. 41, 531 (1969).

[44]Study of the Veneziano model for the $\sigma\pi^+\pi^-\pi^+\pi^-$ five-point amplitude suggested that the $A_1 \to \rho\pi$ decay is nonderivative, i.e., almost pure S-wave (J. Detlefsen, private communication). See also C. A. Savoy, Lett. Nuovo Cimento 2, 870 (1969) [later work on the 6π amplitude has not confirmed this result]; J. D. Dorren, V. Rittenberg, and H. R. Rubinstein, Nucl. Phys. B20, 663 (1970).

[45]D. J. Crennell *et al.*, Phys. Rev. Letters 24, 781 (1970).

[46]J. Ballam *et al.* [Phys. Rev. Letters 21, 934 (1968); Phys. Rev. D 1, 94 (1970)] favor a large D-wave component. In this analysis, a background amplitude having the angular dependence given by one-pion exchange has been subtracted.

[47]I. R. Kenyon *et al.*, Phys. Rev. Letters 23, 146 (1969); N. Armenise *et al.*, Lett. Nuovo Cimento 4, 199 (1970).

[48]D. Cohen *et al.*, University of Rochester report (unpublished).

[49]D. J. Crennell *et al.*, Phys. Rev. Letters 22, 1327 (1969); E. W. Andersen *et al.*, Phys. Rev. Letters 22, 1390 (1969); I. C. Berlinghieri *et al.*, Phys. Rev. Letters 23, 42 (1969); G. Caso *et al.*, Lett. Nuovo Cimento 3, 707 (1970).

[50]M. S. Robin *et al.*, Phys. Rev. Letters 24, 925 (1970); G. Garelick, *Experimental Meson Spectroscopy*, edited by C. Baltay and A. Rosenfeld (Columbia Univ. Press, New York, 1970).

[51]For example, at $s_1 = 1.15$ GeV^2 and $t_2 = -0.1$ GeV^2, we have $-0.07 > t_1 > -0.61$ GeV^2.

[52]F. Gilman *et al.*, Phys. Letters 31B, 387 (1970).

[53]H. Satz, Phys. Letters 32B, 380 (1970).

PHYSICAL REVIEW D VOLUME 5, NUMBER 9 1 MAY 1972

Survey of Inclusive Distributions in a Dual-Resonance Model*

G. H. Thomas
High-Energy Physics Division, Argonne National Laboratory, Argonne, Illinois 60439
(Received 29 December 1971)

From a numerical survey of the dual-resonance model (DRM), it is found that (i) scaling in the central region is approached much more slowly than in the fragmentation regions due partially to kinematics, and partially to the overlap of the two fragmentation regions; (ii) the triple-Regge limit of the model remains a good approximation over most of the fragmentation region, if it is multiplied by a simple modulating factor. The physical origin of such a factor deserves theoretical attention. (iii) If the exchange picture is taken seriously, one should expect wrong-signature-nonsense-zero dips in reactions such as $\pi^- + p \to \pi^0 + X$ for $x \gtrsim 0.2$. The phenomenological implications of the DRM are also discussed.

I. INTRODUCTION

In the past, dual-resonance models (DRM) have provided valuable insights into the structure of scattering amplitudes due to constraints of crossing symmetry, Regge behavior, and narrow-resonance behavior. These insights have been of both a theoretical and phenomenological character.[1] Most recently, attention has been centered on the qualitative application of dual models to inclusive reactions. DeTar, Kang, Tan, and Weis (DKTW)[2] have shown that this model contains many nice theoretical properties, such as limiting behavior in the central and fragmentation regions, triple-Regge asymptotic behavior, and a universal cutoff in transverse momentum of the form $e^{-4\alpha' p_\perp^2}$. A next step would be to study the quantitative applications to data.

Some work of this kind has been done already,[3] and raises many interesting questions concerning the shapes of inclusive distributions one might obtain in the model. To answer such questions, and to investigate further the phenomenological implications, we present in this paper a thorough numerical survey of inclusive shapes in the DRM.

Before proceeding to the numerical study, let us first briefly summarize inclusive reaction terminology.[4] The reaction

$$a + b \to c + X, \tag{1.1}$$

where X represents "anything," can be described in terms of the invariants